Battery-aware energy model of drone delivery tasks

Battery-aware Energy Model of Drone Delivery Tasks

ABSTRACT

Drones are becoming increasingly popular in the commercial market for various package delivery services. In this scenario, the mostly adopted drones are quad-rotors (i.e., quadcopters). The energy consumed by a drone may become an issue, since it may affect (i) the delivery deadline (quality of service), (ii) the number of packages that can be delivered (throughput) and (iii) the battery lifetime (number of recharging cycles). It is thus fundamental try to find the proper compromise between the energy used to complete the delivery and the speed at which the quadcopter flies to reach the destination. In order to achieve this, we have to consider that the energy required by the drone for completing a given delivery task does not exactly correspond to the energy requested to the battery, since the latter is a non-ideal power supply that is able to deliver power with different efficiencies depending on its state of charge.

In this paper, we demonstrate that the proposed battery-aware delivery scheduling algorithm carries more packages than the traditional delivery model with the same battery capacity. Moreover, the battery-aware delivery model is 17% more accurate than the traditional delivery model for the same delivery scheme, which prevents the drone crash.

1. INTRODUCTION

The drone market has recently experienced a significant growth, because of its expansion in the consumer market for commercial and personal use, but also to some regulatory steps, such as the recent action by Federal Aviation Administration (FAA), who granted new exemptions for companies to operate drones in the US [12]. In a scenario in which these devices are used for the delivery of packages, the energy consumption of a drone is a fundamental variable: its proper management affects the quality of service (e.g., meeting delivery deadlines), throughput (number of packages delivered per charge cycle), and also battery health (by reducing the number of charge cycles in a given time horizon). A delivery task requires some time to be executed at a given speed; a faster speed will generally correspond to a larger power demand yet it will decrease delivery time. The actual ''best'' tradeoff between power and performance depends on how they are related. In the case of drones, where the most power consuming device is a rotor, we need to establish a relation between power and energy vs. flight speed. Once such a relation is established, a possibly optimal flight speed could be identified, resulting in various possible scheduling policies for the delivery tasks.

Many works have addressed the scheduling of drone delivery tasks. The main limitation of these works is that they measure electrical power/energy to the motor, which is not exactly in a 1:1 correspondence to battery energy. Two are the reasons for that: (i) the battery is able to deliver power with different efficiencies depending on its state of charge (SoC); (ii) battery power is delivered to the motors trough some conversion process which is not ideal. The first aspect is particularly relevant. In fact, previous works schedule delivery tasks usually adding up the energy demand of each task to determine the aggregate demand; however, the non-linear relation of batteries between available capacity (i.e. energy) and SoC suggests that summing energy may result in inaccurate predictions [1]. Our focus is on the overall model and the methodology to extract these predictions, rather than analyzing complex drone routing/delivery scenarios. Specifically, we show how the SoC-dependent battery efficiency can be incorporated into a usable drone power model, and demonstrate its use on a couple of delivery scenarios.

2. MOTIVATION

According to the flight dynamics of a rotor-based drone, there exists an optimal horizontal speed that minimizes energy consumption, for a given weight (drone + payload) and distance to cover [5, 6, 8]. Figure 1 shows the energy vs. horizontal flight speed curve (dotted) referred to our example quadcopter, for a total weight of 570 grams (100g payload) and a 1 km distance, inclusive of the energy consumption due to take-off and landing.

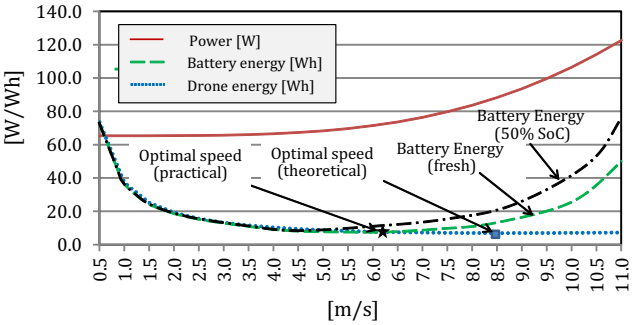

Figure 1: Theoretical and Battery-Aware Energy vs. Speed.

In this example, the energy-optimal (6.96 Wh) speed is 8.5 m/s; however, the curve is virtually constant from about 7.0 m/s on. Therefore, one might be tempted to fly at the maximum speed (11 m/s) since this is a better energy/performance (i.e., delivery speed) tradeoff point. This analysis completely

ignores the fact that this is the energy **required** by the quadcopter, and not the one actually **drawn** from the battery. To explain why this is relevant, the solid curve in the plot shows the *power* consumption at different speeds, which is *monotonically and superlinearly* increasing with speed. This intuitive relation impacts how battery energy is delivered. Since the effective capacity (energy) of a battery is inversely correlated with current demand (the *rate-capacity* effect), larger currents will result in smaller deliverable energy (and this effect is also non-linear). Therefore, it is to be expected that faster speeds will deplete the battery quicker than slower ones. In the example of Figure 1, we should conceptually consider a **battery energy** curve (dashed), which will initially overlap with that of the energy demand (low currents can be efficiently ''served'' by the battery), but will then progressively deviate as speed increases (i.e., larger currents). This will possibly result in an optimal speed which is smaller than the ''ideal'', battery-agnostic one. This speed, in spite of longer flight times, will allow one to complete a larger number of trips before resorting to re-charge.

Furthermore, there is another aspect to be considered: as the SoC of the battery will decrease across different travel legs, its ability to deliver a given current will decrease. This implies that the dashed line in Figure 1 refers to a specific battery SoC. Intuitively, as the SoC decreases, the curve will emphasize its increase in correspondence of higher speeds (dash-dotted line). It is worth emphasizing that the ''battery energy'' curves are just ones to describe the effect; their mathematical derivation is unfeasible, as it would imply expressing the (SoC-dependent) mapping between drone power and battery power as a closed function. This analysis shows that it is essential to bring into a drone power model the actual battery behavior in order to correlate the theoretical energy demand to the actual energy that can be delivered.

3. BACKGROUND AND RELATED WORK

3.1 Quadcopter Dynamics Basics

There are three forces acting on a quadcopter as shown in Figure 2.

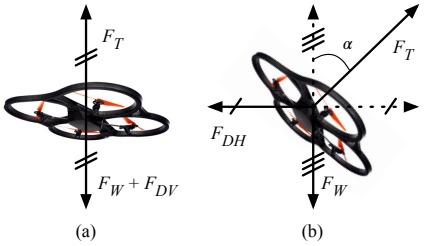

Figure 2: Forces acting on a drone.

Weight (F_W) is a sum of the weight of the drone and payload, which pulls down the drone due to the force of gravity. Drags in horizontal (F_{DH}) and vertical direction (F_{DV}) are forces caused by the disruption of airflow. Drag opposes a movement of the drone in horizontal and vertical directions. Thrust (F_T) is produced by rotating propellers of the drone and opposes the weight and drag to sustain the height and speed of the drone. Figure 2(a) shows the overall forces when a drone flight in vertical direction with a constant speed, and Figure 2(b) shows the overall forces when a drone moves horizontally with a constant speed. The sum of the weight and drag equals to the thrust in both cases.

Weight with a mass of the drone (w_d) and a payload (w_p) and drag with horizontal (v_h) and vertical (v_v) speed are modeled by:

$$F_W = (w_d + w_p)g, F_{DV} = \frac{1}{2}\rho A_t C_d v_v^2, F_{DH} = \frac{1}{2}\rho A_f C_d v_h^2 \quad (1)$$

where g is the gravity, A_f and A_t are cross sectional areas in horizontal and vertical directions, C_d is a drag coefficient, and ρ is air density, respectively. The required thrusts to oppose the weight and drag in vertical and horizontal directions are described as:

$$F_{T,v} = F_W + F_{DV} \text{ and } F_{T,h} = \sqrt{F_W^2 + F_{DH}^2}. \quad (2)$$

Thrust in terms of motor angular speed is modeled by:

$$F_T = \frac{1}{2}\rho A_p C_t (\omega r)^2 \quad (3)$$

where A_p is the disk area of propellers, C_t is a thrust coefficient, ω is angular speed of motors, and r is radius of propellers, respectively. Thrust coefficient obtained with several experiments is from 0.01 to 0.05 [15]. We can easily solve the required thrust for a given drone flight (vertical and horizontal velocities) and payload (payload) from (1)--(2) and the required angular speed to obtain the required thrust from (3).

3.2 Related Work

Many energy-aware path planning algorithms for drones have been proposed in the recent literature. One of the most interesting works ([5]) relies on an experimental model that however does not include the battery performance. In [14], minimum-energy paths for quadrotors are determined after considering the angular accelerations of the propellers, but again not the energy storage properties. In [13], an energy efficient coverage path planning for drones based on Lin-Kernighan heuristic is proposed; however, the related energy model is based only on empirical measurements during the flights of a non-commercial, UB-ANC drone. The routing problem in drone delivery has been analyzed in [6]; however, the proposed power model includes only the weight of the battery, in addition to payload. A comprehensive analysis of the energy consumption of 3D Robotics quadrotor in autonomous missions is reported in [2], after analyzing different maneuvers and velocities. Nevertheless, this is a preliminary study that does truly propose scheduling or routing algorithms. Therefore, when analyzing the relationship between the power consumption of a multirotor, assigned task and available battery energy, generally authors only consider motor power models and possibly a linear characteristic of the energy source, also in the case of delivery analysis [10, 11, 16]. This approach does not take into account the non-linear characteristics of lithium polymer (LiPo) batteries during the discharge phase [17]. That is the reason why predictions of the total overall flight time often are overestimated.

4. DRONE POWER MODEL

The basic equations of the drone forces ((1)-(3)) allow us to derive the required angular speed to sustain the drone (i) at a given height and flying at a constant horizontal speed v_h (ω_h), and (ii) to sustain a constant vertical speed v_v (ω_v),

yielding the following equations:

$$\omega_h = \frac{(4(w_d + w_p)^2 g^2 + \rho^2 A_f^2 C_d^2 v_h^4)^{1/4}}{(r^2 \rho A_p C_t)^{1/2}} = f_h(w_p,\ v_h), \quad (4)$$

$$\omega_v = \frac{(2(w_d + w_p) g + \rho A_t C_d v_v^2)^{1/2}}{(r^2 \rho A_p C_t)^{1/2}} = f_v(w_p,\ v_v). \quad (5)$$

We refer to the drone flight measurement data from [9] where motor current, voltage and angular speed over the drone flight time are specified. The motor current and voltage by angular speed includes the efficiencies of the motor and motor controller. This experimental data was obtained with Parrot AR. Drone 2.0, which has four rotors, and the weight of the drone is 420 g without payload.

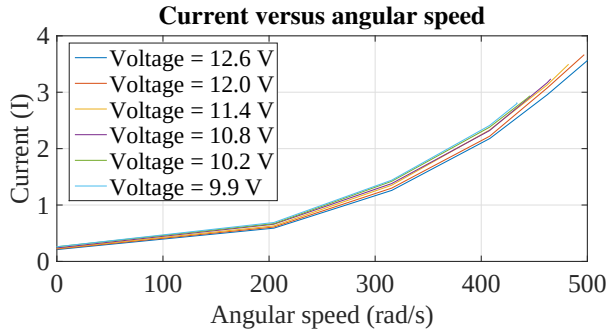

Figure 3: Drone angular speed versus battery power [9].

Figure 3 shows the relationship among the motor angular speed, motor current and voltage. The maximum motor angular speed is 500 rad/s. We empirically fitted the curves to a polynomial, obtaining motor power consumption as

$$P \approx 2.258 \cdot 10^{-07}\omega^3 + 3.866 \cdot 10^{-05}\omega^2 + 5.137 \cdot 10^{-3}\omega + 2.616 = g(\omega). \quad (6)$$

By plugging the expressions of (4)-(6) to (6), we can obtain motor power consumption as a function of payload and speed for the flight both in horizontal direction (P_h) and vertical direction (P_v) as

$$P_h(w_p,\ v_h) \approx g(f_h(w_p,\ v_h)) \quad P_v(w_p,\ v_v) \approx g(f_v(w_p,\ v_v)). \quad (7)$$

4.1 Characterization of a Delivery Task

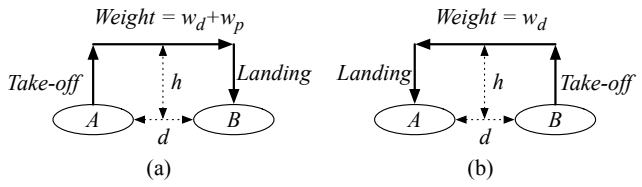

Figure 4: A drone flight model (a) going to place B with a payload and (b) returning to place A without payload.

Figure 4 shows simple drone flight model, which consists of 1) take-off from a place A with constant vertical speed v_v to the height h, 2) flight horizontally during distance d with constant speed v_h and 3) landing with the same vertical speed on a place B. The drone returns to the place A after taking down a package. The overall energy consumption for one delivery is obtained by

$$E \approx P_v(w_p, v_v)\frac{h}{v_v} + P_h(w_p, v_h)\frac{d}{v_h} + P_v(w_p, -v_v)\frac{h}{|-v_v|} + P_v(0, v_v)\frac{h}{v_v} + P_h(0, v_h)\frac{d}{v_h} + P_v(0, -v_v)\frac{h}{|-v_v|}. \quad (8)$$

We assume that the vertical speed for take-off and landing is 3 m/s, which is the maximum vertical speed of AR.Drone 2.0. The height of the drone during horizontal flight is 40 m, which is the 33% of the allowable maximum height to flight the drone in Europe by European Aviation Safety Agency (EASA) [7].

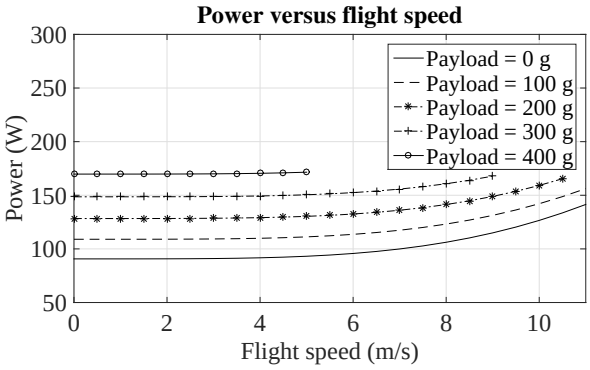

Figure 5: Drone motor power vs. flight speed and payload.

Figure 5 shows the power consumption as a function of horizontal speed and payload. The power consumption at zero horizontal speed coincides with hovering power. The power consumption is almost constant at slow horizontal speeds because the drag is small compared with weight, but quickly increases at faster speeds.

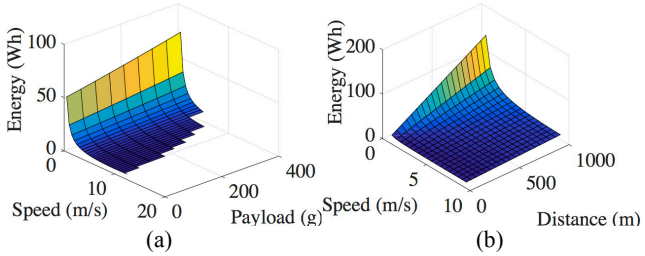

Figure 6: Energy curve (a) when the distance is 500 m and (b) when the payload is 300 g with 100% battery SoC.

Energy for a given delivery task ((8)) is shown in Figure 6. It is a 3-variable function of weight, distance, and flight speed, which is displayed in the figure as two different projections. In general, the maximum horizontal speed decreases with payload because the maximum thrust opposing the weight and drag of the drone is bounded by the maximum motor angular speed. Moreover, there is an energy-optimal horizontal speed for a given delivery task. A drone flight with too slow horizontal speed causes huge energy consumption because the drone consumes most energy to maintain the altitude during the long delivery time. On the other hands, too fast horizontal speed increases drag by the air, which is proportional to the square of the horizontal speed. The energy-optimal speed should be increased as the payload increases in order to reduce the delivery time.

4.2 Battery-Aware Energy Model

The plots of Figures 5--6 are indeed referring to the power and energy *of the drone hardware* and their relation to the relevant quantities (weight, distance, and delivery time, via the flight speed). For an useful evaluation of the actual energy assessment and the feasibility of a given delivery task, however, we need to map the relations descried in Figure 6 onto *battery energy*. As already discussed in Section 2, this require accounting for two issues:*Battery sensitivity to load currents* and *non-ideal conversion efficiency*.

4.2.1 Current-Dependent Battery Efficiency

The fundamental effect to be taken into account is the so-called *rated capacity*: battery effective capacity (equivalent energy) depends on current request. This is normally expressed in battery specs as a voltage/capacity plot, which is typically non-linear. Such non-linearity has a further consequence, that is, as the battery SoC decreases, the battery has virtually a smaller capacity, and therefore a given current depletes a battery more when it is more discharged. Incorporating these effects into our model requires conceptually to project the ''energy'' dimension on the y-axis of Figure 6 onto the ''battery energy'' one. As energy is obtained as the product of power and flight time, mapping drone energy to battery energy cannot be done ''statically'' (i.e., by a direct conversion), but requires *a battery model* that is able to track the energy drawn from the battery by requesting a given current (determined by the flight speed) for a given flight time [4]. Consequently, our power model relies on an offline pre-characterization phase described in Section 4.2.3.

4.2.2 Conversion Efficiency

The power (voltage/current) level required to operate the drone hardware should be adapted the power level of the battery pack that supplies it. This is carried out by a non-ideal DC/DC converter whose efficiency can be a complex function of the involved quantities. More specifically. assuming a switching converter, the efficiency is mainly affected by the difference in input/output voltages and the load current [2]. The latter in particular is relevant - efficiency degrades for small load currents. In this work, we assume a constant efficiency and neglect such dependencies. The main reason for that simplifying assumption, besides simplicity, is that we want to emphasize the first effect in this work. Nevertheless, our framework could easily incorporate a current-dependent efficiency.

4.2.3 Construction of the Power Model

The power model consists of a 5-dimensional table that is built offline according to the flow described in Figure 7. The table stores all possible values of battery SoC drop in response to a given delivery task.

We have to build the battery energy by actually building the *power profile* of a given delivery task (i.e., as in Figure 4). Although a delivery task is fundamentally defined only by payload weight and distance, we need to consider also al possible speeds to determine the actual power waveform. In Line 1--4 we thus build all possible power profiles for each combination of valid weight, distance, and horizontal speed; this yields a waveform $P(t)_{|w=w_i,d=d_i,v=v_i}$[1]. This includes

[1]As already discussed, ve assume a fixed vertical speed of 3 m/s

```
1.  foreach weight w_i ∈ [0, w_max]
2.    foreach speed v_i ∈ [v_min, v_max]
3.      foreach distance d_i ∈ [d_min, d_max]
4.        calculate P_|w=wi,d=di,v=vi (t)          // Figure 4
5.        calculate I_batt(t) = P_|w=wi,d=di,v=vi (t) /(η · V_batt(t))
6.        foreach SOC level SOC_i ∈ [10,100]
7.            calculate ΔSOC_i by applying I_batt(t) to the
              battery model and store it in T[w_i, d_i, v_i, SOC_i]
8.      endfor
9.    endfor
10.  endfor
11. endfor
```

Figure 7: Offline Model Characterization.

take-off, the first leg to the target, landing, take-off, second leg to the base, and landing.

Since $P(t)$ is the drone power profile, we need to translate it into battery power; this is simply done by rescaling power with respect to the efficiency factor of the converter (Line 5). Notice that battery voltage is considered as constant. This yields a current waveform $I_{batt}(t)$. From this derivation it is evident how the assumption of a constant efficiency is not a limitation - a more complex function can be used here without substantial modification in the process.

We then apply (Line 7) this current profile to a simulation model of the battery. In this work we use the one by [4], in which a traditional circuit-equivalent model of [3] is extended in such a way that it can track the SOC depletion based on the dynamics of the current profile. We adopted this model because it allows to track the decrease of SOC of the battery for a given current profile. The amount of consumed SoC is then stored into the table $\mathbf{T}$, which represents the actual model.

$\mathbf{T}$ is a 5-dimensional table that returns the decrease of battery SOC resulting from a drone delivery over a distance d_i, carrying a payload with weight w_i, at a speed v_i, and for a battery having an SOC SoC_i at the beginning of the delivery. The computational cost of build the model is obviously determined by the discretization interval for the various quantities. For building function $E()$, the cost is $O(|W| \cdot |D| \cdot |V| \cdot |S|)$, where $|W|, |D|, |V|$ and $|S|$) are the number of discretized levels of weights, distances, speeds, and SOC, respectively. In our case we have $|W| = 4$ (min/max payload =100/400g, step = 100g), $|D| = 10$ (min/max distance = 100/1000m, step = 100m), $|V| = 11$ (min/max speeds 1-11 m/s, step 1m/s), and $|S| = 10$ (min.max SOC=10%-100%; the calculation involves therefore 4400 invocations of the battery model of [4], each requiring a fraction of a second. The total characterization time with the above discretization step is in the order of approximately 10 minutes.

4.2.4 Usage of the Power Model

Given $\mathbf{T}$, the simulation of a sequence of delivery tasks is relatively straightforward. The only computation involved is the calculation of the optimal flight speed.

Given a task τ_a with payload w_a and delivery distance d_a, and the current battery SOC SoC_a (100% for the first task), we extract the projection $\mathbf{T}(v)_{|w=w_a,d=d_a,SoC=SoC_a}$ of $\mathbf{T}$ describing the the ΔSoC corresponding to the triple $w = w_a, d = d_a, SoC = SoC_a$, and where speed is left as the only free variable.

On this single variable function We then simply search of the speed value $v_{opt,a}$ that yields the smallest $\Delta SoC_a =$

$min_v \mathbf{T}(v)_{|w=w_a, d=d_a, SoC=SoC_a}$; this will be the optimal battery-aware flight speed.
The next task τ_b, say, with payload w_b and delivery distance d_b, will be executed assuming an initial SOC $\text{SoC}_b = \text{SoC}_a - \Delta\text{SoC}_a$. The optimal speed v_b and the minimum ΔSoC_b are thus obtained as describe above, and the process is repeated for all tasks in the task set.

5. SIMULATION RESULTS

5.1 Simulation Setup

We selected the *Parrot AR.Drone 2.0* device, since there are comprehensive measurement data available in [9], which allows us to build the drone power consumption model. Concerning the battery, we used the *Ultimate PX-04 LIPO Battery*; Table 1 indicates the manufacturer's data of this battery. We used a battery pack of 5000 mAh at 11.1 V nominal voltage. We assumed a constant converter efficiency of 90%.

Table 1: Manufacturer's parameters of the selected battery.

Parameters	Ultimate PX-04 LIPO
Rated Capacity	1000 mAh
Nominal Voltage	11.1 V
Cut-off voltage	9.0 V

5.2 Delivery Task Battery-aware Scheduling

In order to show how the proposed battery-aware energy model can be applied in a general framework involving a set of delivery tasks, we formulated a couple of scenarios related to the scheduling of a set of drone deliveries. This makes it possible to analyze how the proposed model can solve the inaccuracies of ignoring the battery non-ideal behavior when using the traditional model.
In this context, a number n of delivery tasks $\{\tau_1, ...\tau_n\}$ have to be carried out by a given drone. Each delivery $\tau_i = (w_i, d_i)$ is characterized by a payload weight w_i and a distance d_i from the base station to the delivery target. We assumed that only one package is delivered for each task. Unlike other approaches (e.g., [16], in which batteries are immediately recharged after delivering one single package, we assumed that the drone delivers packages until its battery is almost fully discharged.
Although this scenario might be somehow improved through other more involved variants (e.g., time constraints), it is generated just for the purpose of demonstrating the effectiveness of the proposed energy model.

5.2.1 Comparison of Different Schedulings

In this experiments, we generated two sets of delivery tasks with different payloads and distances, whose specific values are shown in Table 2. Notice that these two sets are opposed one to each other: set A has the longest distance with the heaviest payload, and the shortest distance with the lightest paylaod, whereas set B has the opposite situation.
There are 6 different tasks to be delivered one by one in each set; the total number of possible scheduling orders is 720. Due to the space limitation, here we report the best and worst cases only, since all the other results are located between these two cases. In this context, *best case* means that all the tasks are delivered with the minimum energy and, therefore, there is still available capacity in the battery, whereas *worst case* means that the drone cannot finish all the delivery tasks because the battery is fully depleted. In terms of set A, we found that the best scheduling is $F \rightarrow E \rightarrow B \rightarrow D \rightarrow C \rightarrow A$, while the worst scheduling is the mirrored one.

Table 2: Delivery tasks for Set A and Set B.

	Set A		Set B	
Task	**W (g)**	**D (m)**	**W (g)**	**D (m)**
A	100	100	300	100
B	200	100	400	100
C	100	200	400	200
D	100	300	400	300
E	200	500	200	500
F	400	900	100	900

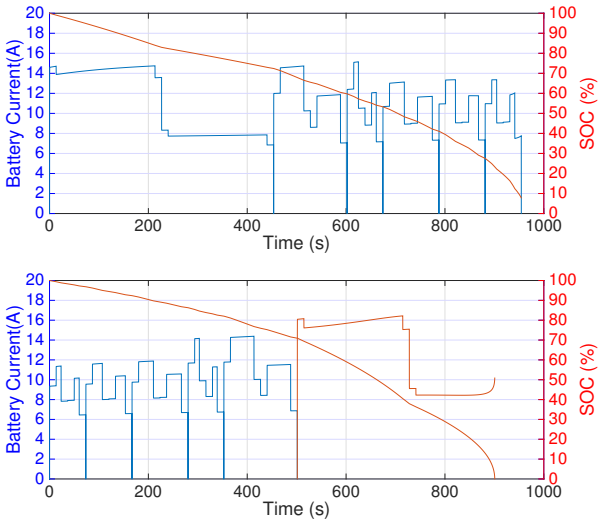

Figure 8: Best and worst scheduling of set A.

Figure 8 shows the battery current and SOC during delivering all the tasks of set A. The upper sub-figure corresponds to the best scheduling case: the battery SOC is 7.81% after delivering all the tasks. On the other hand, in the worst scheduling case they cannot be all accomplished before the battery is exhausted, as shown in the bottom sub-figure. Notice that, at constant power, the discharge current increases dramatically at the ending phase because the battery voltage decreases evidently at low SOC. This is determined by the non-linear characteristics of the battery behavior. It is also the reason why the current provided by battery for task F in the worst scheduling case is slightly higher than the one in the best scheduling case. Concerning set B, we got a similar result. In this case, the best scheduling is $D \rightarrow B \rightarrow C \rightarrow A \rightarrow E \rightarrow F$, whereas the worst scheduling is the opposite one.
Notice that the best scheduling policy always starts with the task having the heaviest payload and longest distance. In fact, since the battery is more efficient in *serving* larger current requests when fully charged, an effective scheduling policy would be *heaviest-longest-first*. There is an interesting parallel with the well-known property of battery-aware

scheduling of tasks in a processor, in which executing tasks in decreasing order of current demand is probably optimal.

5.2.2 *Using the Model as an Accurate Predictor*

Since the current demand is directly correlated with the total weight, the optimal scheduling policy can be determined in advance. In order to analyze how many tasks can be really accomplished, we used the scheduling policy *heaviest-and-longest-first* on the task set described in Table 3, and then we compared the results of the proposed energy model against the classical one.

Table 3: Delivery tasks with various payloads and distances.

Task	Weight (g)	Distance (m)
A	300	100
B	100	200
C	400	300
D	300	400
E	400	600
F	200	900

In this case, the optimal scheduling is $E \rightarrow C \rightarrow D \rightarrow A \rightarrow F \rightarrow B$. Figure 9 shows that, the residual battery SOC is estimated at 15% after delivering all the tasks when considering the traditional model, whereas the battery is indeed nearly fully discharged during the delivery of task B using a battery-aware model.

In practice, there is a difference in the estimation of the battery SOC of about 17% when considering the two models, as indicated by the dotted line in Figure 9. Therefore, in this case the proposed model can really suggest the right decision weather or not to start delivery task B, while the traditional model makes the drone landing (at very low SOC for safety reasons) unexpectedly before accomplishing this task, as a consequence of overestimating the *effective* capacity of the battery.

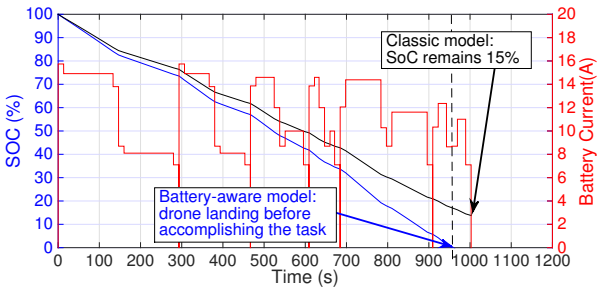

Figure 9: Comparison of the models.

6. CONCLUSIONS

Package delivery services operated with drones are becoming popular. In order to guarantee the quality of the provided service it is fundamental properly characterize the energy consumed by the drones. Existing works target the delivery tasks scheduling problem without considering a fundamental factor: the battery is a non-ideal power supply that delivers power depending on its state of charge. Hence, the energy required by the drone for completing an assigned delivery task may not correspond to the energy requested to the battery. This means that, if the battery SoC is not accounted, predictions of the total overall flight time may be overestimated. In this paper we demonstrated this estimation inaccuracy and we showed how the SoC-dependent battery efficiency can be incorporated into a usable drone power model.

7. REFERENCES

[1] Aleksandrov, D., and Penkov, I. Energy consumption of mini UAV helicopters with different number of rotors. In *11th International Symposium Topical Problems in the Field of Electrical and Power Engineering* (2012), pp. 259--262.

[2] Chang, K., Rammos, P., Wilkerson, S. A., Bundy, M., and Andrew Gadsden, S. LiPo battery energy studies for improved flight performance of unmanned aerial systems. In *Proceedings Volume 9837, Unmanned Systems Technology XVIII.* (2016), pp. 98370W0--W10.

[3] Chen, M., and Rincón-Mora, G. Accurate electrical battery model capable of predicting runtime and IV performance. *IEEE Transactions on Energy Conversion 21*, 2 (2006), 504--511.

[4] Chen, Y., Macii, E., and Poncino, M. A circuit-equivalent battery model accounting for the dependency on load frequency. In *Proceedings of the Conference on Design, Automation & Test in Europe (DATE)* (2017), pp. 1177--1182.

[5] Di Franco, C., and Buttazzo, G. Energy-aware coverage path planning of UAVs. In *2015 IEEE International Conference on Autonomous Robot Systems and Competitions (ICARSC)* (2015), pp. 111--117.

[6] Dorling, K., Heinrichs, J., Messier, G. G., and Magierowski, S. Vehicle routing problems for drone delivery. *IEEE Transactions on Systems, Man, and Cybernetics: Systems 47*, 1 (January 2017), 70--85.

[7] European Aviation Safety Agency (EASA). Opinion No 01/2018 --- Introduction of a regulatory framework for the operation of unmanned aircraft systems in the 'open' and 'specific' categories. https://www.easa.europa.eu/sites/default/files/dfu/Opinion%20No%2001-2018.pdf, 2018.

[8] Goss, K., Musmeci, R., and Silvestri, S. Realistic Models for Characterizing the Performance of Unmanned Aerial Vehicles. In *Proc. 26th International Conference on Computer Communication and Networks (ICCCN)* (2017), pp. 1--9.

[9] Jeurgens, N. L. M. Implementing a Simulink controller in an AR.Drone 2.0. DC 2016.005, Eindhoven University of Technology, January 2016.

[10] Lee, L. Optimization of a modular drone delivery system. In *2017 Annual IEEE International Systems Conference (SysCon)* (April 2017), pp. 1--8.

[11] Lim, J., and Jung, H. Drone delivery scheduling simulations focusing on charging speed, weight and battery capacity: Case of remote islands in South Korea. In *2017 Winter Simulation Conference (WSC)* (December 2017), pp. 4550--4551.

[12] Meola, A. Drone market shows positive outlook with strong industry growth and trends. http://www.businessinsider.com/drone-industry-analysis-market-trends-growth-forecasts-2017-7?IR=T, 13 July 2017.

[13] Modares, J., Ghanei, F., Mastronarde, N., and Dantu, K. UB-ANC Planner: Energy Efficient Coverage Path Planning with Multiple Drones. In *Proc. 2017 IEEE International Conference on Robotics and Automation (ICRA)* (2017), pp. 6182--6189.

[14] Morbidi, F., Cano, R., and Lara, D. Minimum-Energy Path Generation for a Quadrotor UAV. In *2016 IEEE International Conference on Robotics and Automation (ICRA)* (2016), pp. 1492--1498.

[15] Newman, S. *The foundations of helicopter flight.* Halsted Press, 1994.

[16] Park, S., Zhang, L., and Chakraborty, S. Battery assignment and scheduling for drone delivery businesses. In *2017 IEEE/ACM International Symposium on Low Power Electronics and Design (ISLPED)* (2017).

[17] Podhradský, M., Coopmans, C., and Jensen, A. Battery state-of-charge based altitude controller for small, low cost multirotor unmanned aerial vehicles. *Journal of Intelligent & Robotic Systems 74*, 1-2 (2014), 193--207.